Characterization of the Oligomeric States of Wild Type and Mutant AraC†

Nicole LaRonde-LeBlanc‡ and Cynthia Wolberger*,‡,§

Howard Hughes Medical Institute and Department of Biophysics and Biophysical Chemistry, Johns Hopkins University School of Medicine, 725 North Wolfe Street, Baltimore, Maryland 21205-2185

Received June 1, 2000; Revised Manuscript Received July 20, 2000

ABSTRACT: AraC regulates transcription of the *Escherichia coli* arabinose operon, binding tandem DNA half-sites in the presence of arabinose and widely spaced half-sites in the absence of arabinose. In the structure of the AraC N-terminal dimerization domain with bound arabinose, the protein dimerizes via an antiparallel coiled-coil interface. The absence of bound ligand opens a second, β-barrel interaction interface that also mediates interactions between unliganded AraC dimers in the crystal. The larger buried surface area of the β-barrel interface, as compared with the coiled-coil interface, raised the possibility that protein−protein interactions mediated by the β-barrel might play a role in ligand-mediated modulation of AraC DNA binding activity. For the crystallographically observed β-barrel interaction to play a role in the cell, dimerization via this interface in the absence of arabinose would be predicted to be at least as energetically favorable as dimerization via the coiled-coil interface. In the study presented here, we use analytical ultracentrifugation to determine the oligomeric state of the AraC dimerization domain in the presence and absence of arabinose. Dimerization of the unliganded protein via the β-barrel interface in the absence of interactions mediated by the coiled-coil interface is assayed using a mutant AraC protein with a disrupted coiled-coil interface. The results of these studies indicate that dimerization via the β-barrel interface is substantially weaker than dimerization via the coiled-coil interface, indicating that the crystallographically observed β-barrel interaction is not relevant to in vivo function.

The AraC protein regulates the *Escherichia coli* arabinose operon, araBAD, by contacting different combinations of DNA binding sites in response to the presence or absence of the sugar L-arabinose (*1*). In the absence of arabinose, a single AraC dimer contacts two half-sites separated by more than 200 base pairs, looping out the intervening DNA and repressing the pBAD promoter (*1*−*5*). Upon binding arabinose, the protein dimer binds to two closely spaced half-sites, resulting in activation of pBAD (*4*−*6*). The ability of arabinose to act as an inducer of transcriptional activation is blocked by D-fucose, which is a competitive inhibitor of AraC (*7*−*9*). The 292-residue AraC protein contains two apparently independent domains that are connected by a flexible linker made up of about five residues (*10*−*12*). The N-terminal domain of AraC (residues 1−167) binds arabinose and mediates dimerization, while the C-terminal domain (residues 178−292) binds DNA (*10*). The N-terminal domain alone is capable of mediating an arabinose response, as seen by the ability of a chimeric protein containing the N-terminal domain of AraC fused to a LexA DNA binding domain to respond to arabinose (*10*). A central question is how arabinose modulates the DNA binding activity of AraC, converting it from a protein dimer that loops DNA to one that favors binding to closely spaced sites.

The structure of the N-terminal domain of AraC (*13*) revealed several features thought to be important to the mechanism of arabinose-mediated switching of AraC binding site preferences (Figure 1). Arabinose binds to AraC in a pocket located within a β-barrel (Figure 1A). The N-terminal arm of the protein (residues 7−18) folds over the sugar, burying it within the binding pocket. AraC with bound arabinose crystallizes as a dimer, with the C-terminal α-helixes from each of two monomers associating to form an antiparallel coiled-coil interface (Figure 1B). A mixture of van der Waals and hydrogen bonding interactions stabilizes the dimer. Leu150 and Leu151 of one monomer interact with Leu161 of the opposing monomer to form a leucine triad at each end of the coiled coil, while in the center of the interface, a buried water mediates hydrogen bonds with Asn154 and Gln158 of both monomers. In addition, Asn154 forms hydrogen bonds with Glu157 (Figure 1B). In the structure of AraC determined in the absence of arabinose (*14*), the overall features of the protein are similar except that the lack of bound sugar leads to a disordering of 12 N-terminal arm residues (residues 7−18). This exposes the sugar binding pocket in the unliganded structure and allows the β-barrels of adjacent proteins in the crystal to interact with one another, thereby forming a second dimerization interface (Figure 1C). This β-barrel interface buries 75% more surface area (2100 Å^2) than the coiled-coil interface (1200 Å^2). Additional favorable interactions are formed by Tyr31, which inserts into the sugar binding pocket of the opposing monomer and packs against the indole ring of Trp95. The β-barrel and coiled-coil interfaces are structurally independent and are both available to mediate dimerization

† Supported by the Howard Hughes Medical Institute.

* To whom correspondence should be addressed: Department of Biophysics and Biophysical Chemistry, Johns Hopkins University School of Medicine, 725 N. Wolfe St., Baltimore, MD 21205-2185. Phone: (410) 955-0728. Fax: (410) 955-0637. E-mail: cwolberg@jhmi.edu.

‡ Department of Biophysics and Biophysical Chemistry.

§ Howard Hughes Medical Institute.

10.1021/bi001262g CCC: $19.00
Published on Web 08/25/2000

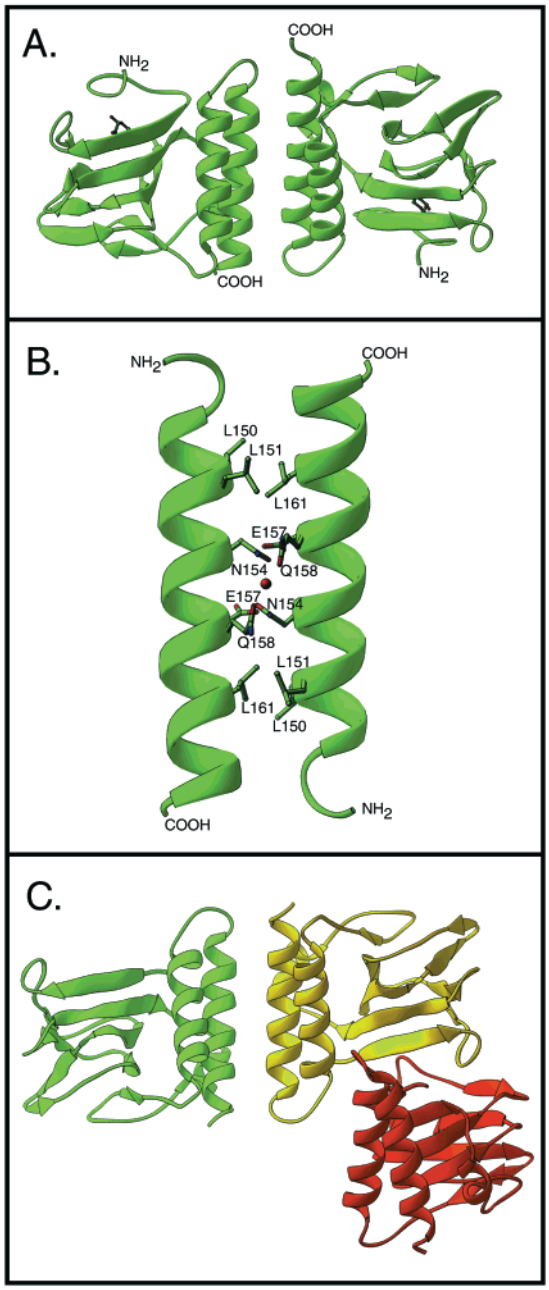

FIGURE 1: Dimerization interfaces of AraC. (A) AraC dimer with bound arabinose dimerizing via the coiled-coil interface. (B) A detailed view of the side chain interactions at the coiled-coil interface. (C) The structure of AraC in the absence of arabinose, showing the interaction between the three AraC monomers as they are packed in the crystal. The central monomer shown in yellow interacts with one monomer (red) via the coiled-coil β-barrel interface and with the other (green) via the coiled-coil interface.

in the absence of arabinose. When arabinose binds to AraC, the filling of the sugar binding pocket and folding of the N-terminal arm over the sugar close off the β-barrel interface, leaving only the coiled-coil interface to mediate dimerization.

The AraC protein has been shown to bind DNA as a dimer in both the presence and absence of arabinose (for a review, see ref *15*). While the form of the AraC dimer with bound arabinose is clear, only one of the two potential dimer interfaces seen in the crystals of AraC in the absence of arabinose can be the relevant one in solution. Structural studies of other oligomeric proteins have indicated that the interface in the crystal with the largest buried surface area is the biologically relevant one (*16*), which raised the possibility that the larger, β-barrel interface is responsible for mediating dimerization of the unliganded AraC protein (*13*). This led to the proposal of a dimerization-switch model, which postulates that AraC dimerizes via the β-barrel interface in the absence of arabinose and through the coiled-coil interface in the presence of arabinose (*13*). The proposed switch in dimerization interfaces would result in a change in the relative distance between the DNA binding domains within a single AraC dimer, since dimerization via the β-barrel interface places the C-terminal DNA binding domain attachment points 60 Å apart, as compared with 37 Å in the coiled-coil dimer (*13*). A change in the relative positions of the DNA binding domains could account, in part, for the different binding site spacing preferences of the liganded and unliganded AraC protein. For the dimerization-switch model to be plausible, association via the β-barrel interface must be energetically favored over that via the coiled-coil interface, since both interfaces are available in the absence of arabinose. An alternate model has been proposed (*17*) in which the N-terminal arm of AraC, which is freed in the absence of arabinose, contacts the DNA binding domains and constrains them in a way that promotes binding to widely separated sites and DNA looping. This proposal has been made on the basis of mutagenesis and biochemical studies, as there is no structural information about the intact AraC protein in either the presence or absence of arabinose.

The aim of this study was to test the dimer-switch model by characterizing in solution the intermolecular self-association of AraC mediated by the coiled-coil and β-barrel interfaces. A tryptic fragment of the AraC protein containing residues 2−178, which includes the dimerization domain, was studied in the analytical ultracentrifuge. Using sedimentation velocity and equilibrium analytical ultracentrifugation, studies of the oligomeric state of the AraC N-terminal domain were carried out in the presence and absence of arabinose and in the presence of fucose. On the basis of observations from the crystal structure (*13*), it was expected that higher-order oligomers should be observed in solution in the absence of arabinose due to self-association via two independent interfaces, while in the presence of arabinose, only coiled-coil dimers should be observed. Sedimentation velocity experiments reported previously (*13*) and in the study presented here indicate the presence of dimers and higher-order species in the absence of arabinose, but only a single homogeneous dimer in the presence of arabinose. Sedimentation equilibrium data collected on AraC in the presence and absence of arabinose did not indicate the presence of a significant concentration of AraC monomers, indicating that the arabinose-bound AraC dimer is highly stable under the conditions that were studied.

To assay interactions mediated by the β-barrel interface, site-directed mutagenesis was used to produce mutants deficient in association through the coiled-coil interface. If AraC were indeed capable of dimerizing using the β-barrel interface, protein defective in dimerization via the coiled-coil interface would be expected to be monomeric in the presence of arabinose but dimeric in the absence of arabinose. Mutations were designed to disrupt the leucine triad at each end of the interface and the water-mediated hydrogen bond interactions at the center of the coiled coil (Figure 1B). Four side chain substitutions were required to completely disrupt

interactions mediated by the coiled-coil interface: Leu150 and Leu151 to Lys, Asn154 to Ala, and Leu161 to Ser. The quadruple-mutant AraC protein was shown to be completely monomeric in the presence of arabinose by both size-exclusion chromatography and sedimentation velocity analytical ultracentrifugation. Contrary to the prediction of the dimerization-switch model, this mutant was also monomeric in the absence of arabinose, indicating an absence of dimerization through the beta-barrel interface. These results together indicate that the coiled-coil interface is the interface utilized by the protein for dimerization in both the absence and presence of arabinose in solution. Our findings rule out a model in which arabinose controls a switch between dimerization interfaces, but are consistent with models that invoke changes in the conformation of the AraC N-terminal arm as the source of the switch in DNA binding site preferences of AraC (*17*).

EXPERIMENTAL PROCEDURES

Protein Expression and Purification. The wild-type AraC N-terminal domain was expressed from plasmid ARACTF4 (A. VanDemark and C. Wolberger, unpublished results) which contains the DNA coding sequence for residues 1−182 of AraC inserted into the *Nde*I and *Avr*II sites of pET21b (Novagen). This construct results in the expression of the AraC N-terminal domain fused to a histidine tag at the protein's C-terminus. A triple mutant (L150K/L151K/N154A) was produced by PCR-mediated site-specific mutagenesis using ARACTF4 as a template. The forward primer 5′-GAGATATACATATGGCTG-3′ contains a 5′-*Nde*I site. The reverse primer 5′-CAGTAACAATTGCTCAAGCAGAGCTATCGCCTTCTTCTCCGAATA-3′ contains the mutations (underlined) and a *Mun*I site. The resulting PCR product was cut with *Nde*I and *Mun*I and ligated into the ARACTF4 plasmid that had been cut with the same enzymes. The quadruple mutant (L150K/L151K/N154A/L161S) was produced by site-directed mutagenesis with the Stratagene Quik-Change Mutagenesis kit using oligonucleotides 5′-CGGAGCTGCTGGCGATAAATCTGCTTGAGCAATTG-3′ and 5′-GCCTCGACGACCGCTATTTAGACGAACTCGTTAAC-3′ on the plasmid containing the triple mutant coding sequence. DNA sequencing was used to confirm the presence of the mutations. The proteins were overexpressed in *E. coli* BL21(DE3) [F^- *omp*T $r_B^-mB^-$(DE3)]. Cells containing the plasmids were grown at 37 °C in LB medium containing 80 μg/mL carbenicillin to an OD_{600} of 0.6−1.0. The temperature was then lowered to 30 °C, and the cells were induced with 1 mM IPTG for 3 h. Cells were harvested by centrifugation and stored at −80 °C until they were used. Cells were lysed in 50 mM NaH_2PO_4 (pH 8.0), 300 mM NaCl, 0.2% arabinose, 0.1% igepal, 0.1% β-mercaptoethanol, 10 mM imidazole, and 1 mg/mL lysozyme. The His-tagged protein was affinity purified on Ni−agarose resin from Qiagen using solutions (modified to contain 0.2% arabinose) and methods outlined in the manufacturer's insert. The resulting >90% pure protein was dialyzed into 25 mM Tris (pH 8.0), 100 mM KCl, and 0.1% arabinose and digested with 0.1% w/w trypsin to cleave the residues C-terminal to Arg178, thereby removing the histidine tag. Incubation times for enzymatic cleavage at 4 °C were 16−20 h for the wild type and 4−6 h for the mutant protein. Further purification to >98% homogeneity was achieved by anion exchange chromatography on a Pharmacia Mono Q column equilibrated in 15 mM Tris (pH 8.0), 25 mM KCl, and 0.2% arabinose and eluted with a gradient of 25 to 825 mM KCl over 10 column volumes. The molecular mass of the purified protein was confirmed by mass spectrometry. The protein preparation was stored at 4 °C and dialyzed into the appropriate buffer prior to being used in experiments.

Size-Exclusion Chromatography. Size-exclusion chromatography was performed at 4 °C on a Pharmacia Superdex 75 HR 10/30 column equilibrated in 15 mM Tris (pH 8.0), 150 mM KCl, and 0.2% arabinose at a flow rate of 0.5 mL/min. The column was calibrated using albumin (67 kDa), ovalbumin (43 kDa), chymotrypsin (25 kDa), and ribonuclease A (14 kDa) as molecular mass standards. The protein preparations of wild-type and mutant AraC proteins were dialyzed into the column buffer and diluted to approximately 0.6 mg/mL, and 1.2 mL was injected onto the column. Protein elution was monitored by absorbance at 280 nm.

Circular Dichroism Spectroscopy. Protein was exchanged into 20 mM sodium phosphate buffer (pH 8.0) using a Pharmacia 5 mL Fast Desalt column and diluted to a final concentration of 1 mg/mL. Circular dichroism spectra were collected on an AVIV DS60 spectrometer at 20 °C using a 0.1 mm path length cuvette. For each spectrum, an average of multiple scans (six for the wild type and nine for the quadruple mutant) was collected from 185 to 260 nm at 0.5 nm increments. Microsoft EXCEL was used to subtract buffer and cell contributions and convert the spectra to molar ellipticity.

Analytical Ultracentrifugation. Analytical ultracentrifugation experiments were carried out in a Beckman Optima XLI instrument at 20 °C using optical absorption detection at a wavelength of 280 nm. Protein samples were transferred into the appropriate buffer using a Pharmacia 5 mL fast desalting column or by dialysis immediately prior to ultracentrifugation runs. Buffers contained 20 mM Tris (pH 8.0) and 75 mM KCl with or without 0.2% (w/v) arabinose with or without 0.2% (w/v) fucose. Sedimentation velocity experiments were carried out in an An 60 Ti rotor at 60 000 rpm using 1.2 cm (when OD < 1.2) and 0.3 cm (when OD > 1.2) two-sector charcoal-filled Epon centerpieces with quartz windows. Each sample was monitored for 50−60 scans recorded at least 5 min apart. Sample concentrations were 0.3, 0.6, and 1.5 mg/mL for each protein. Sedimentation equilibrium experiments were carried out in six-channel charcoal-filled Epon centerpieces with quartz windows at speeds of 12 000, 15 000, 21 000, 26 000, 28 000, 32 000, and/or 35 000 rpm. Equilibrium was reached after 18−20 h, as determined by comparing scans taken at 2 h intervals beginning at 10 h. Equilibrated scans were used for analysis.

Sedimentation Velocity Data Analysis. Sedimentation coefficients corrected for diffusion were calculated for each boundary by the method of van Holde and Weischet (*18*), and the boundary fraction versus the $S_{20,W}$ was plotted to show the distribution of sedimentation coefficients in the sample. Each boundary was divided into 50 fractions. The 50−60 scans collected for each cell were edited and analyzed using Ultrascan (provided by B. Demeler, University of Texas Health Sciences Center at San Antonio, San Antonio, TX). The partial specific volumes were 0.73 cm^3/g for the AraC N-terminal domain and 0.73 cm^3/g for the quadruple

mutant, as calculated from the amino acid sequence. The buffer density was 1.0022 g/cm^3 as calculated from buffer components excluding arabinose and fucose. The partial specific volume and buffer density were calculated using Ultrascan.

Sedimentation Equilibrium Data Analysis. Equilibrium data were edited and analyzed by nonlinear least-squares fitting of primary absorbance data using the Windows 95 version of the NONLIN algorithm (*19*). All data were initially analyzed for average molecular mass using a model for a single ideal species:

$$c_r = c_{r_0} \exp[\sigma(\xi_r - \xi_{r_0})] + \delta Y$$

where c_r is the concentration of protein monomer at a given radial position r, c_{r_0} is the concentration at a reference position r_0, $\sigma = M(1 - \upsilon\rho)\omega^2/RT$ (where M is the monomer molecular mass, υ is the partial specific volume, ρ is the buffer density, ω is the angular velocity, R is the universal gas constant, and T is the absolute temperature in kelvin), $\xi_r = r^2/2$, $\xi_{r_0} = r_0^2/2$, and δY is the correction term for a non-zero baseline. The data were then fit in terms of a monomer−dimer equilibrium to the equation

$$c_r = c_{r_0} \exp[\sigma(\xi_r - \xi_{r_0})] + (c_{r_0})^2 K_{a,2} \exp[2\sigma(\xi_r - \xi_{r_0})] + \delta Y$$

where $K_{a,2}$ is the association constant for the dimer. The data obtained with the wild-type protein in the absence of arabinose were also fit to a dimer−tetramer model using the above equation with σ substituted by 2σ. The best fit was determined by minimization of the variance, and the quality of fit was determined by examination of the residuals.

RESULTS

Oligomeric States of the Wild-Type AraC N-Terminal Domain in the Absence of Arabinose. The crystallographic data on AraC suggest that two independent dimerization interfaces exist when the protein is not bound to arabinose. Higher-order oligomers would therefore by expected to form in solution as a consequence of simultaneous interactions through the two interfaces. To verify this, velocity sedimentation experiments were performed using the wild-type AraC protein in the absence of arabinose. Velocity sedimentation data were subjected to van Holde−Weischet analysis, which provides a proven method of determining the species homogeneity of protein solutions (*18*, *20*). This method was employed to determine the oligomeric state of the purified 20.5 kDa AraC N-terminal domain (residues 1−178) in the absence of arabinose. Plots of the boundary fraction versus $S_{20,W}$ generated from this analysis of the sedimentation velocity data detected a heterogeneous mixture in the absence of arabinose with species ranging from 3.2 to 4.7 S (Figure 2A),[1] in agreement with previously reported data (*13*). In a comparison of results obtained at protein concentrations of 0.3, 0.6, and 1.5 mg/mL, the level of higher-order species was higher with increasing concentrations (Figure 2A). As a way of collecting shape-independent information about the AraC oligomeric species in solution, sedimentation equilibrium experiments were performed to obtain an estimate of the molecular mass of the protein in the absence of arabinose. The weight-averaged molecular mass, obtained from the sedimentation equilibrium data using a single-species model, was 42.7 ± 1.7 kDa (variance$^{1/2} = 9.9 \times 10^{-3}$) (Figure 3A). Use of a monomer−dimer or a dimer−tetramer model resulted in no significant further randomization of the residuals or improvement in the goodness of fit. It was therefore concluded that in the absence of arabinose, there is slight oligomerization to yield higher-order species as evidenced by the velocity data, but that the protein is mainly dimeric as shown through the equilibrium data. The dissociation constant for the higher-order species must be weaker than 0.1 mM, as judged by the inability to fit the data to higher-order dissociation models.

Oligomeric State of Wild-Type AraC N-Terminal Domain in the Presence of Arabinose. The binding of arabinose to AraC closes off the β-barrel interface, leaving only the coiled-coil interface available for dimerization. As shown in Figure 2B, as well as in previous experiments (*13*), velocity sedimentation data from samples to which arabinose has been added do not exhibit species heterogeneity. In the study presented here, arabinose was added directly to the sample that had been studied by velocity sedimentation in the absence of arabinose, indicating that the aggregation observed without arabinose is reversible. The purified AraC N-terminal domain sediments as a single homogeneous species of 3.2 S, which corresponds to a dimer, in the presence of 0.2% arabinose at 0.3, 0.6, and 1.5 mg/mL (Figure 2B). Sedimentation equilibrium experiments were performed in the presence of arabinose to provide a shape-independent confirmation of this result. The weight-averaged molecular mass obtained by sedimentation equilibrium experiments was 37.2 ± 1.5 kDa (variance$^{1/2} = 9.4 \times 10^{-3}$) using a single-species model (Figure 3B). Attempts to fit the data to a monomer−dimer model resulted in no further randomization of the residuals.

In vivo data indicate that fucose acts as a competitive inhibitor of AraC (*7*−*9*). Sedimentation velocity studies were performed using the AraC N-terminal domain to observe the effects of equal amounts of arabinose and fucose on the protein's oligomeric state. Under these conditions, which would result in inhibition of AraC activation in vivo, the AraC N-terminal domain sediments as a single homogeneous dimeric species of 3.2 S (Figure 2C) as seen in the presence of arabinose only. These results show that fucose does not affect the oligomeric state of AraC under the conditions that were studied.

Oligomeric States of the Mutated AraC N-Terminal Domain. If oligomerization via the β-barrel interface is to play a role in the cell, the strength of interactions mediated by this interface must be comparable to those mediated by the coiled-coil interface. Since both interfaces are available in the absence of arabinose, it was necessary to disrupt the coiled-coil dimerization interface to allow independent measurement of dimerization via the β-barrel interface. The mutant AraC N-terminal domain with a disrupted coiled-coil dimerization interface would be expected to be monomeric in the presence of arabinose. In the absence of

[1] Abbreviations: WT, wild type; KKA, *E. coli* AraC protein (residues 1−178) with Leu150 and Leu151 to Lys and Asn154 to Ala mutations; KKAS, *E. coli* AraC protein (residues 1−178) with Leu150 and Leu151 to Lys, Asn154 to Ala, and Leu161 to Ser mutations; K_d, equilibrium dissociation constant.

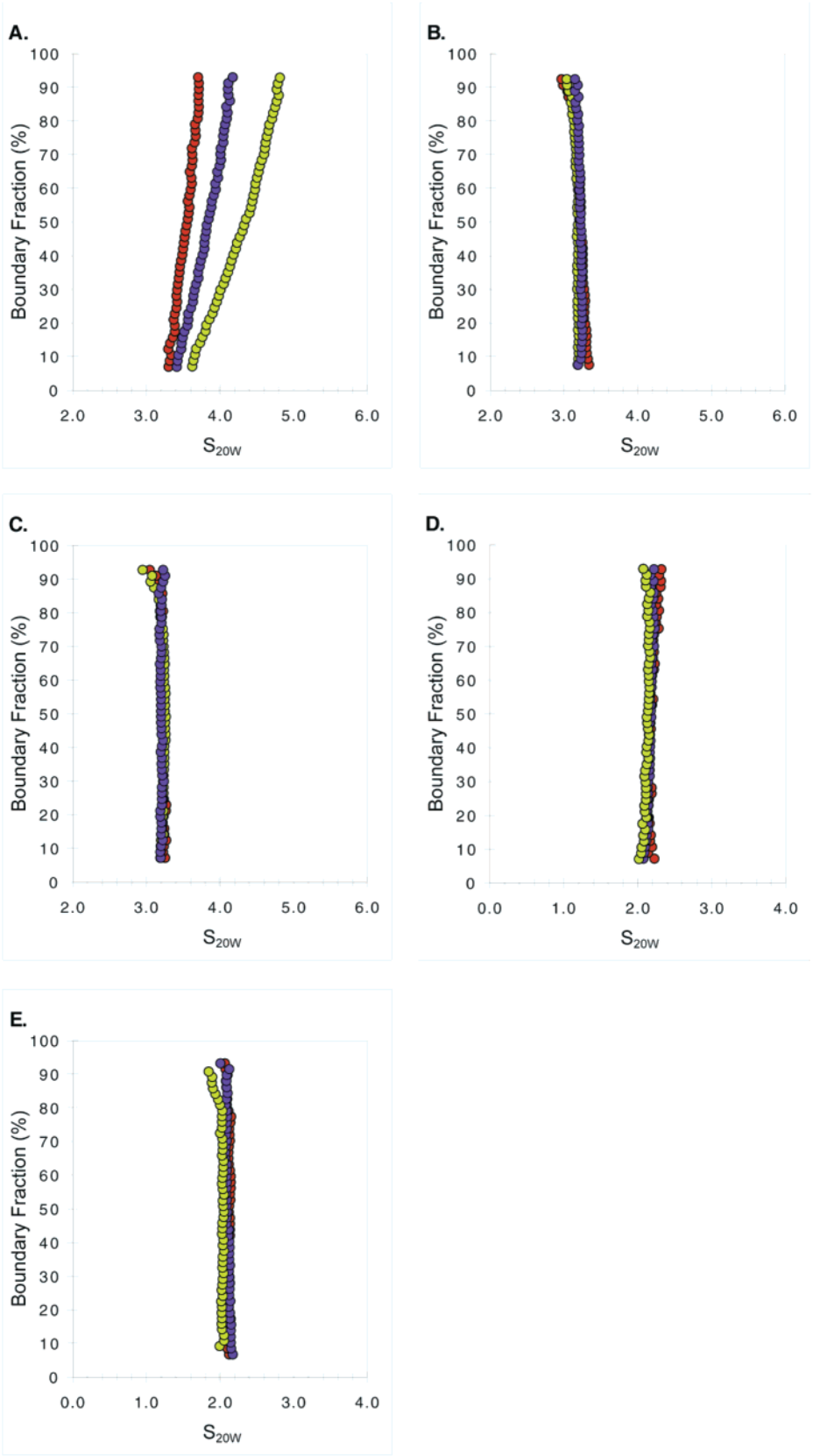

FIGURE 2: Velocity sedimentation data on the wild-type AraC N-terminal domain and the quadruple mutant analyzed by the method of van Holde and Weischet (*18*, *20*). (A) WT AraC N-terminal domain with no added arabinose. (B) WT AraC with 0.2% (w/v) arabinose. (C) WT AraC with 0.2% arabinose and 0.2% fucose. (D) Quadruple mutant (L150K/L151K/N154A/L161S) with no added arabinose. (E) Quadruple mutant with 0.2% arabinose. The plots were generated using 280 nm absorbance data collected at 60 000 rpm in buffer containing 75 mM NaCl at pH 8.0 for each sample. All plots were made using Ultrascan (red, 0.3 mg/mL; blue, 0.6 mg/mL; yellow, 1.5 mg/mL).

arabinose, any dimer formation would presumably result from interactions mediated by the β-barrel interface. Using the structure of the AraC N-terminal domain as a guide, key residues responsible for stabilizing the coiled-coil dimeriza-

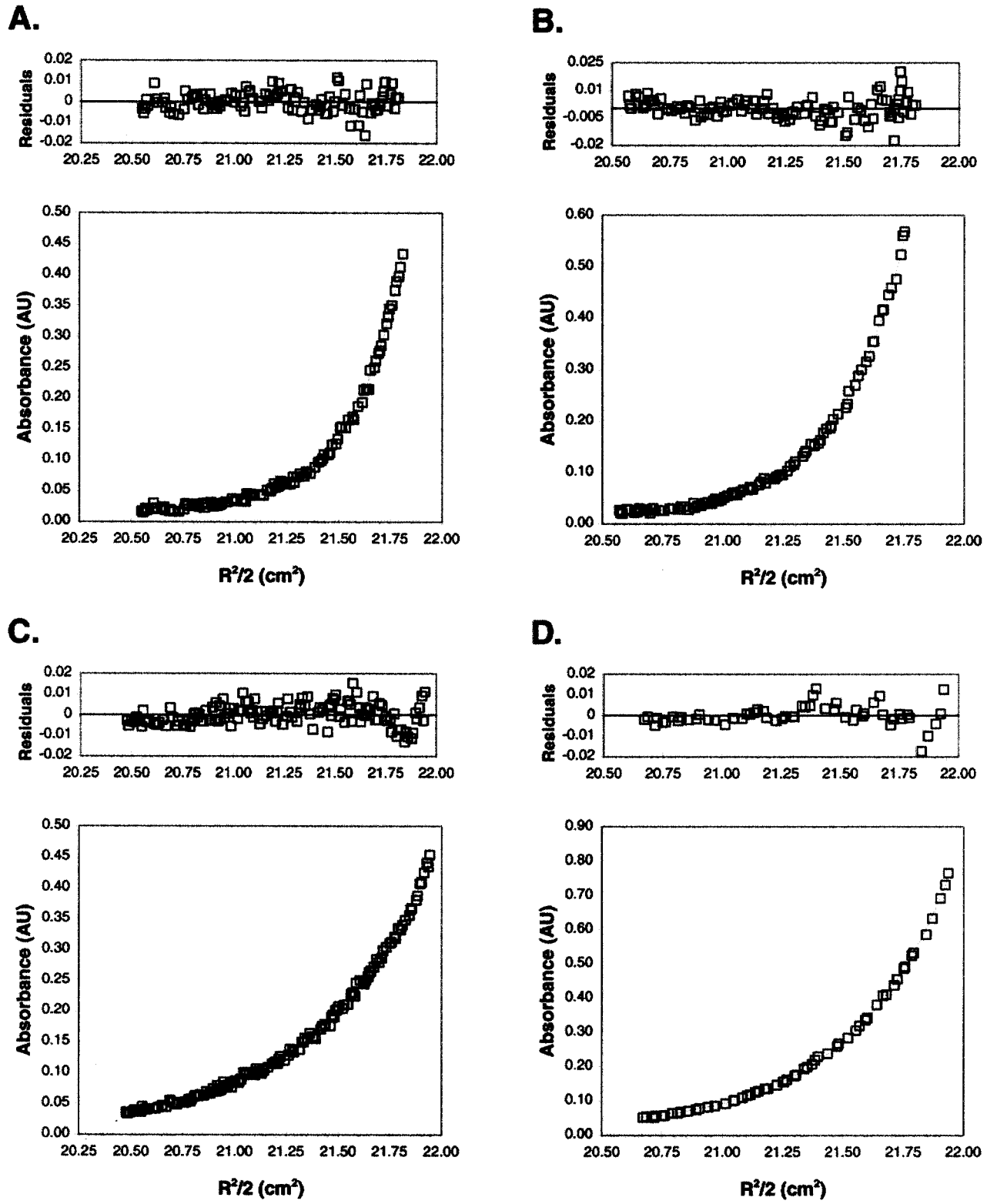

FIGURE 3: Sedimentation equilibrium data for AraC wild-type N-terminal domain and the quadruple mutant. Fitted data and residuals for one of 15 data files used in fitting a single species model for (A) the WT AraC N-terminal domain with no added arabinose (data obtained at 28 000 rpm, 0.15 mg/mL), (B) WT AraC with 0.2% (w/v) arabinose (data obtained at 28 000 rpm, 0.15 mg/mL), (C) the quadruple mutant (L150K/L151K/N154A/L161S) with no added arabinose (data obtained at 28 000 rpm, 0.15 mg/mL), and (D) the quadruple mutant with 0.2% arabinose (data obtained at 32 000 rpm, 0.15 mg/mL). The *x*-axis is (radial position $r)^2/2$. Data were collected at 280 nm and fit using NONLIN for Windows 95 (*19*).

tion interface were substituted with residues designed to disrupt protein−protein interactions. Initially, three mutations were introduced at the coiled-coil interface. Residues Leu150 and Leu151 were substituted with lysine to disrupt the leucine triad at each end of the antiparallel coiled coil, and Asn154 was changed to alanine to disrupt the hydrogen bonding network at the center of the coiled coil (Figure 1B). Size-exclusion chromatography was performed in the presence of arabinose using triple-mutant and wild-type AraC proteins (Figure 4).The wild-type AraC protein migrates as a species

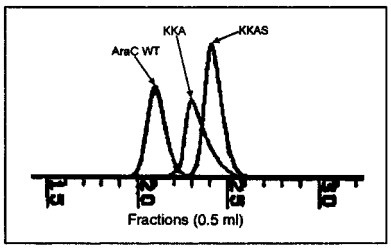

FIGURE 4: Size-exclusion chromatography of the wild-type AraC N-terminal domain and mutants. The WT AraC N-terminal domain (20.5 kDa), the triple mutant (KKA) (L150K/L151K/N154A), and the quadruple mutant (KKAS) (L150K/L151K/N154A/L161S) were injected separately onto a Superdex 75 size-exclusion column, with elution monitored by UV absorbance at 280 nm. The resulting chromatograms were overlaid to show differences in elution profiles. The protein molecular masses obtained from a standard curve were 38.9 kDa for WT AraC, 18.9 kDa for KKAS, and 25.0 kDa for KKA. The absorbance at 280 nm is plotted along the *y*-axis, and the *x*-axis indicates fraction numbers (where one fraction is 0.5 mL).

with a molecular mass of 38.9 kDa, which is close to the calculated dimer molecular mass of 41.0 kDa. However, the chromatogram of the triple-mutant protein corresponds to a protein with a molecular mass of 25.0 kDa, which is intermediate between the monomer (20.5 kDa) and dimer molecular masses. This is consistent with sedimentation velocity analysis of the triple mutant in the presence of arabinose, which indicates the presence of a mixture of monomers and dimers (data not shown). These results strongly suggested that the three mutations (L150K, L151K, and N154A) did not succeed in completely disrupting dimerization via the coiled-coil interface.

Introduction of a fourth mutation was required to completely disrupt dimerization mediated by the coiled-coil interface. This side chain substitution, which replaces Leu161 with serine, removes the third leucine from the leucine triad located at each end of the antiparallel coiled coil. The AraC N-terminal domain containing all four mutations (L150K, L151K, N154A, and L161S) migrates on a gel filtration column as a species with a molecular mass of 18.9 kDa, which is very close to the predicted value of 20.5 kDa (Figure 4). Sedimentation velocity experiments of the quadruple mutant in the presence of 0.2% arabinose at 0.3, 0.6, and 1.5 mg/mL revealed a single monomeric species of 2.1 S (Figure 2D), consistent with the size-exclusion chromatography results. These results confirm that the four mutations completely disrupt dimerization via the coiled-coil interface under the conditions used in this study. Sedimentation equilibrium experiments were performed on the quadruple mutant to provide a shape-independent confirmation of these findings. The resulting data are consistent with the sedimentation velocity results and fit well to a single-species model with an averaged molecular mass of 19.9 $\pm$ 1 kDa (variance$^{1/2}$ = 4.3 $\times$ 10^{-3}) in the presence of arabinose (Figure 3C).

It was not possible to assay AraC size-exclusion chromatography in the absence of arabinose due to interaction of the AraC protein with the column matrix in the absence of its ligand. Analytical ultracentrifugation assays were therefore carried out on the mutant AraC protein in the absence of arabinose to determine whether interactions mediated by the open β-barrel interface could be detected. Sedimentation velocity experiments carried out at protein concentrations of 0.3, 0.6, and 1.5 mg/mL indicate the presence of a single

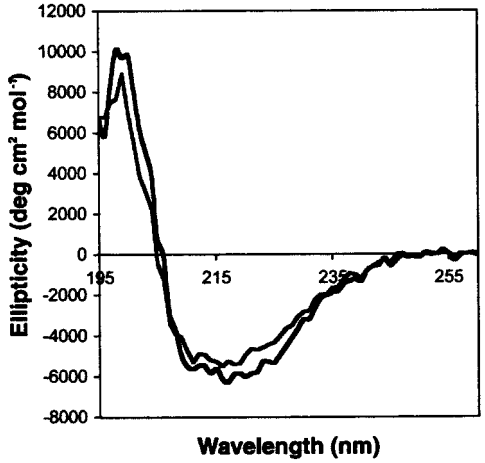

FIGURE 5: Circular dichroism spectra of the wild-type AraC N-terminal domain and the quadruple mutant. Far-UV CD spectra of the AraC N-terminal domain (black line) and the quadruple mutant (gray line) were recorded to compare the secondary structure of the two proteins.

monomeric species of 2.1 S (Figure 2E). No evidence of any significant protein aggregation is evident in the van Holde−Weischet analysis of the data. Similarly, sedimentation equilibrium data on the mutant protein in the absence of arabinose fit well to a single-species model with a weight-averaged molecular mass of 20.1 $\pm$ 1 kDa (variance$^{1/2}$ = 7.5 $\times$ 10^{-3}) (Figure 3D). These results indicate that, in the absence of a functional coiled-coil dimerization interface, no dimerization of the AraC N-terminal domain occurs under the solution conditions used here even when the β-barrel interface is available due to the absence of arabinose. To rule out the possibility that the mutations may have led to incorrect protein folding, thereby affecting the ability of the mutant protein to interact via the β-barrel interface, circular dichroism (CD) spectra of the wild-type and quadruple-mutant protein were recorded in the absence of arabinose (Figure 5). No significant differences in the CD spectra were observed, indicating that the substitutions did not have a notable effect on the protein's secondary structure. Moreover, the sensitivity of the mutant protein to protease digestion is indistinguishable from that of the wild type (data not shown), further indicating that the protein fold is not disrupted by the mutations. The lack of dimerization of the mutant protein in the absence of arabinose, when the β-barrel interface is available, indicates that there is no interaction via the β-barrel interface in this mutant under the conditions used in this study.

DISCUSSION

This study was designed to test whether the extensive β-barrel interface observed in crystals of the AraC N-terminal domain in the absence of arabinose mediates interactions of sufficient strength to play a role in gene regulation. A key test was the complete disruption of the coiled-coil interface by multiple mutations, thereby allowing the independent assay of potential interactions mediated by the β-barrel interface. Four mutations in the coiled-coil interface were required to completely disrupt dimerization via the coiled-coil interface, converting the AraC N-terminal domain into a monomer in the presence of arabinose. We find that in the absence of arabinose, the quadruply mutated protein is also

monomeric (2.1 S), indicating that no significant protein−protein interactions are mediated by the β-barrel interface under the conditions that were tested. If interactions mediated by the β-barrel interface were at least as strong as those at the coiled-coil interface, dimers of the quadruple-mutant protein should have been observed in the absence of arabinose. While it is quite possible that AraC proteins interact through the β-barrel interface at higher protein concentrations, the strength of these interactions would be too weak to be relevant in the cell, where the concentration of the AraC protein has been estimated to be 1×10^{-8} M (*21*). Our findings therefore rule out the dimer-switch model, which requires the β-barrel interface to be at least as strong as, or stronger than, the coiled-coil interface.

This study, as well as a previous report (*13*), documents that the wild-type AraC protein in the absence of arabinose forms a dimer with some residual formation of higher-order multimers. In light of our mutant studies, the dimers found in the absence of arabinose must be formed by the coiled-coil interface, as is the case in the presence of arabinose. The aggregation of AraC in the absence of arabinose may be mediated by the N-terminal arm, the β-barrel, or other parts of the protein. This aggregation does not lead to formation of a significant number of higher-order species, as evidenced by the fact that it was not possible to fit the equilibrium ultracentrifugation data to dissociation models for formation of higher-order multimers. These interactions must have a K_d of >0.1 mM, which is the limit of detection in the assays that were used, and are therefore too weak to play any likely role in gene regulation in the cell. Since no self-association is detected in the quadruply mutated AraC protein, the interactions that give rise to slight aggregation of the wild-type protein must depend on prior formation of the coiled-coil dimer.

In the analysis of contacts between proteins observed in the crystalline environment, the relative amount of protein surface area buried upon complex formation is the common method of identifying biologically relevant protein−protein interaction interfaces (*16*). Since more buried surface area has been associated with greater binding affinity, these criteria led to the proposal that the β-barrel interface of AraC would mediate stronger protein−protein interactions than the coiled-coil interface. However, the β-barrel interaction is clearly shown not to be the stronger interaction interface in the experiments described here. While we cannot completely rule out the possibility that mutations in the coiled-coil region diminish the strength of interactions mediated by the β-barrel interface, the distance between the two interfaces makes this highly unlikely, as does the fact that the CD spectrum of the mutated protein does not differ from that of the wild-type protein. The observation of reversible aggregation by the AraC N-terminal domain in the absence of arabinose may mean that the β-barrel interaction can occur weakly in solution when the interface is available. However, the strength of this interaction would be insufficient to be consistent with the dimer-switch model, leading us to conclude that this does not constitute a likely mechanism for arabinose-regulated DNA binding by AraC. Our results provide a striking counter example to the commonly accepted use of buried surface area as an indicator of relative strength of macromolecular interactions.

The results reported here are consistent with the alternate, "light-switch" model that has been proposed as a mechanism for modulation of the AraC protein DNA binding activity by arabinose (*17*). According to that model, AraC dimerizes exclusively via the coiled-coil interface, with arabinose serving as a ligand that modulates the conformation of the N-terminal arm of the protein. While the N-terminal arm binds to arabinose in the liganded protein, the absence of arabinose frees the N-terminal arm of AraC to bind to the DNA binding domain. The binding of the arm is postulated to constrain the DNA binding domain in an orientation that causes the AraC dimer to favor binding to the widely spaced I1 and O2 sites, thereby looping out the intervening DNA. Supporting this model is the observation that deletions and point mutations in the N-terminal arm that include residues 7−15 result in arabinose-independent activation of pBAD by AraC (*17*). Furthermore, random mutagenesis of the C-terminal DNA binding domain produced mutants that were not activated by arabinose, but whose arabinose responsiveness could be restored by introducing second-site mutations in the N-terminal arm (*17*). Further biophysical studies using the full-length AraC protein in the presence and absence of arabinose and in the presence of fucose will be needed to probe the proposed differences in protein conformation, yielding a clearer picture of the mechanism.

ACKNOWLEDGMENT

We thank A. VanDemark for the AraC protein expression vector and purification protocols, E. Sprague for help with analytical ultracentrifugation data collection, J. Hansen for assistance with data interpretation, B. Demeler for the use of Ultrascan and training in data analysis, and R. Schleif and J. Aishima for comments on the manuscript.

REFERENCES

1. Hendrickson, W., and Schleif, R. (1985) *Proc. Natl. Acad. Sci. U.S.A. 82*, 3129−3133.
2. Wilcox, G., and Meuris, P. (1976) *Mol. Gen. Genet. 145*, 97−100.
3. Dunn, T. M., Hahn, S., Ogden, S., and Schleif, R. F. (1984) *Proc. Natl. Acad. Sci. U.S.A. 81*, 5017−5020.
4. Martin, K., Huo, L., and Schleif, R. F. (1986) *Proc. Natl. Acad. Sci. U.S.A. 83*, 3654−3658.
5. Lobell, R. B., and Schleif, R. F. (1990) *Science 250*, 528−532.
6. Zhang, X., Reeder, T., and Schleif, R. (1996) *J. Mol. Biol. 258*, 14−24.
7. Beverin, S., Sheppard, D. E., and Park, S. S. (1971) *J. Bacteriol. 107*, 79−86.
8. Doyle, M. E., Brown, C., Hogg, R. W., and Helling, R. B. (1972) *J. Bacteriol. 110*, 56−65.
9. Wilcox, G. (1974) *J. Biol. Chem. 249*, 6892−6894.
10. Bustos, S. A., and Schleif, R. F. (1993) *Proc. Natl. Acad. Sci. U.S.A. 90*, 5638−5642.
11. Eustance, R. J., Bustos, S. A., and Schleif, R. F. (1994) *J. Mol. Biol. 242*, 330−338.
12. Eustance, R. J., and Schleif, R. F. (1996) *J. Bacteriol. 178*, 7025−7030.
13. Soisson, S. M., MacDougall-Shackleton, B., Schleif, R., and Wolberger, C. (1997) *Science 276*, 421−425.
14. Soisson, S. M., MacDougall-Shackleton, B., Schleif, R., and Wolberger, C. (1997) *J. Mol. Biol. 273*, 226−237.
15. Schleif, R. (1996) in *Escherichia coli and Salmonella typhimurium* (Niedhardt, R. F. C., III, Inagraham, J., Lin, E., Low,

K., Magasanik, B., Reznikoff, W., Riley, M., Schaechter, M., and Umbarger, H., Eds.) pp 1300−1309, American Society for Microbiology, Washington, DC.
16. Janin, J., and Rodier, F. (1995) *Proteins 23*, 580−587.
17. Saviola, B., Seabold, R., and Schleif, R. F. (1998) *J. Mol. Biol. 278*, 539−548.
18. Van Holde, K. E., and Weischet, W. O. (1978) *Biopolymers 17*, 1387−1403.
19. Johnson, M. L., Correia, J. J., Yphantis, D. A., and Halvorson, H. R. (1981) *Biophys. J. 36*, 575−588.
20. Demeler, B., Saber, H., and Hansen, J. C. (1997) *Biophys. J. 72*, 397−407.
21. Kolodrubetz, D., and Schleif, R. (1981) *J. Mol. Biol. 149*, 133−139.

BI001262G